

Upconversion enhancement in $\text{NaYF}_4:\text{Yb}^{3+}, \text{Er}^{3+}$ crystal via Bi^{3+} doping

S X Xiao, Z S Chen*, H Q Huang, J G Zheng and J P Xu

Jiangxi Key Laboratory for Mass Spectrometry and Instrumentation, East China University of Technology, Nanchang, Jiangxi 330013, P.R. China

Email: zhshcheng@ecit.cn

Abstract. In this research, $\text{NaY}_{0.8-x}\text{F}_4:18\%\text{Yb}^{3+}, 2\%\text{Er}^{3+}, x\%\text{Bi}^{3+}$ ($x = 0, 1, 2, 4, 7, 10\text{mol}\%$) crystals were prepared by a simple hydrothermal method. Their purity process and upconversion (UC) intensity were controlled by different amounts of Bi^{3+} doping. The intensity of UC red and green emission were enhanced by 5.5 and 4.9 folds respectively at 4 mol% Bi^{3+} doping.

1. Introduction

Rare earth-doped upconversion (UC) luminescence is based on two-photon or multi photon mechanism of the long-wave radiation into fluorescent material shortwave radiation, which contains the anti-Stokes luminescence properties^[1]. UC materials are widely used in the fields of biological imaging^[2], 3D printing^[3], sensors^[4] and solar cell^[5] because of their good chemical stability, optical stability and less toxicity. However, the low efficiency of conversion hinders its further development^[6].

From the perspective of the crystal, the UC luminescence of $\text{NaYF}_4:\text{Yb}^{3+}, \text{Er}^{3+}$ crystal is mainly depend on the transition of Er^{3+} energy levels to produce different UC emission, but the luminescence properties of Er^{3+} are strongly affected by the surrounding environment of crystal^[7]. In theory, the asymmetry of the crystal environment is easy to make Er^{3+} f-f resonance transitions^[8], so the change amount of some ions in $\text{NaYF}_4:\text{Yb}^{3+}, \text{Er}^{3+}$ crystals can achieve this purpose^[9]. The regulation of heterogeneous ion doping on the luminescence properties of $\text{NaYF}_4:\text{Yb}^{3+}, \text{Er}^{3+}$ crystal plays a very important role. Different kinds of heterogeneous ion doping enhances UC luminescence intensity by changing the distance of interplanar spacing and the electron cloud density of the crystal which affect the distance between the luminescence center and the energy transfer center^[10].

Various heterogeneous ions, such as $\text{Li}^+, \text{Mn}^{2+}, \text{Ca}^{2+}, \text{Ba}^{2+}, \text{Zn}^{2+}$, have been doped to enhance UC intensity^[11]. To the best of our knowledge, however, the effect of Bi^{3+} doping on the UC properties has not been reported yet. Herein, a series of Bi^{3+} doped $\text{NaYF}_4:\text{Yb}^{3+}, \text{Er}^{3+}$ were fabricated via a simple hydrothermal method. The influence of Bi^{3+} doping has been discussed in detail.



2. Experiment

1 mmol nitrates contained Y^{3+} , Yb^{3+} , Er^{3+} and Bi^{3+} in a ratio of $(80-x):18:2:x$ ($x=0\sim 10$), 1.2g NaOH, 10 mL OA, and 10 mL ethanol were added into a 40 ml of Teflon-line autoclave under vigorous stirring for 30 min, 4 mmol NH_4F was dissolved in distilled water and added in the former liquid dropwise and heated at $200^\circ C$ for 24 h in muffle furnace. The samples were cooled down to room temperature and concentrated by a centrifuge with deionized water and ethanol to wash for three times, respectively. The final products were drying at $60^\circ C$ for 24 h to collect the powders.

The crystalline structure of as-obtained samples was determined by X-ray diffraction (XRD, D/ruax2550PC, Tokyo, Japan) using CuK_α radiation ($\lambda = 0.154056$ nm) over a 2θ range from 10° to 80° at a scanning rate of $4^\circ/\text{min}$. The morphology of the particles was performed by the scanning electron microscope (SEM, Nova Nano SEM 450, FEI) operating at an acceleration voltage of 200 kV after a gold spray process. The UC emission spectra were recorded by a spectrophotometer (Hitachi F-4500, Tokyo, Japan) equipped with a power-controllable 980 nm diode laser (LOS-BLD-0980-C Hite photoelectric, China).

3. Results and discussion

Figure.1(a) shows when the concentration of Bi^{3+} is free and 1 mol%, there is a small amount of cubic phase, and when the concentration of Bi^{3+} is more than 1 mol%, the pure hexagonal is produced. It can be inferred that the doping of Bi^{3+} is helpful to produce pure hexagonal $NaYF_4:Yb^{3+}$, Er^{3+} crystal. However, it shifted from an obvious peak to a smaller angle that can be observed by amplified an angle of 43° the peak of (201) in Figure.1(b)

According to Bragg's law^[12]:

$$2d\sin\theta = n\lambda.$$

Combined with the angle shift in Figure.1(a), when the diffraction angle is lower, the space between the ions in the lattice is larger. That is to say, the lattice plane spacing becomes larger with the doping of Bi^{3+} . This is because the Bi^{3+} radius ($r_{Bi} = 0.103$ nm) is larger than that of the Y^{3+} ($r_Y = 0.089$ nm)^[13], so the introduction of Bi^{3+} will lead to the volume expansion of the $NaYF_4:Yb^{3+}$, Er^{3+} crystal, when the crystal plane spacing becomes larger and the peak value shifts to 42° .

It is shown that Bi^{3+} doping $NaYF_4:Yb^{3+}$, Er^{3+} crystal, only played a role in the substitution because of no indication that the peak is shifted to 42° and then move reversely in Figure.1(b).

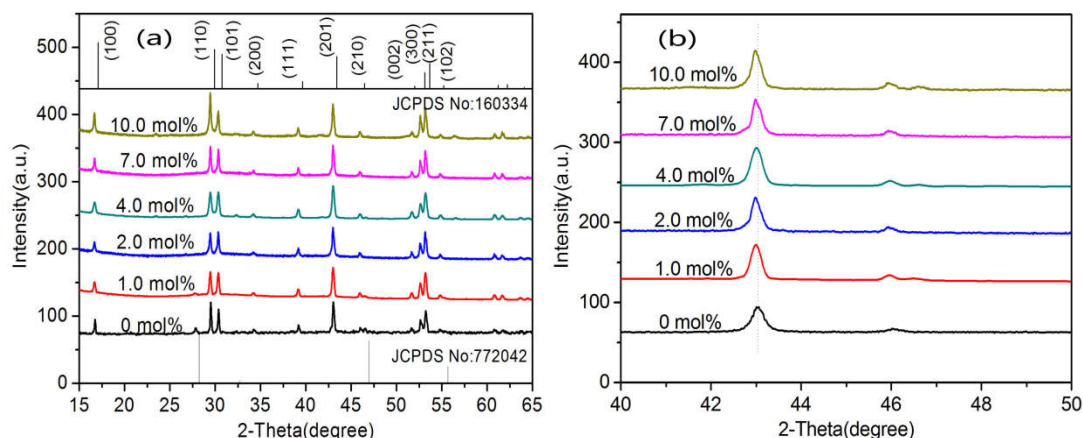


Figure. 1 XRD patterns of (a): $NaY_{0.8-x}F_4:18\%Yb^{3+}$, $2\%Er^{3+}$, $x\%Bi^{3+}$ ($x = 0, 1, 2, 4, 7,$

10mol%)products, standard XRD pattern of hexagonal NaYF_4 (JCPDS No.16-0334), and (b): amplified of the main diffraction peaks (201) at 43° from Figure.1(a).

The SEM images showed the different amount of Bi^{3+} doped in $\text{NaYF}_4:\text{Yb}^{3+}$, Er^{3+} crystals in the Figure.2. In Figure 2(a) and (b) showed the presence of micro-rods and nanoparticles, the length of the micro-rods in the range of 600 ~ 800 nm, while the morphology of nanoparticles is not very uniform. According to the results of XRD, the Bi^{3+} -free and 1 mol% Bi^{3+} sample are cubic and hexagonal phase, the other samples are almost pure hexagonal phase. It can be considered that the nanoparticles are cubic phase and the micro-rods particles are hexagonal. And in Figure 2(c)~(f), most of nanoparticles have been converted into micro-rods and their length is ranged from 600 to 800 nm. The results showed that the substitution of low concentration ($\text{Bi}^{3+}=1\sim 10\text{mol}\%$) does not change the crystal morphology drastically^[14].

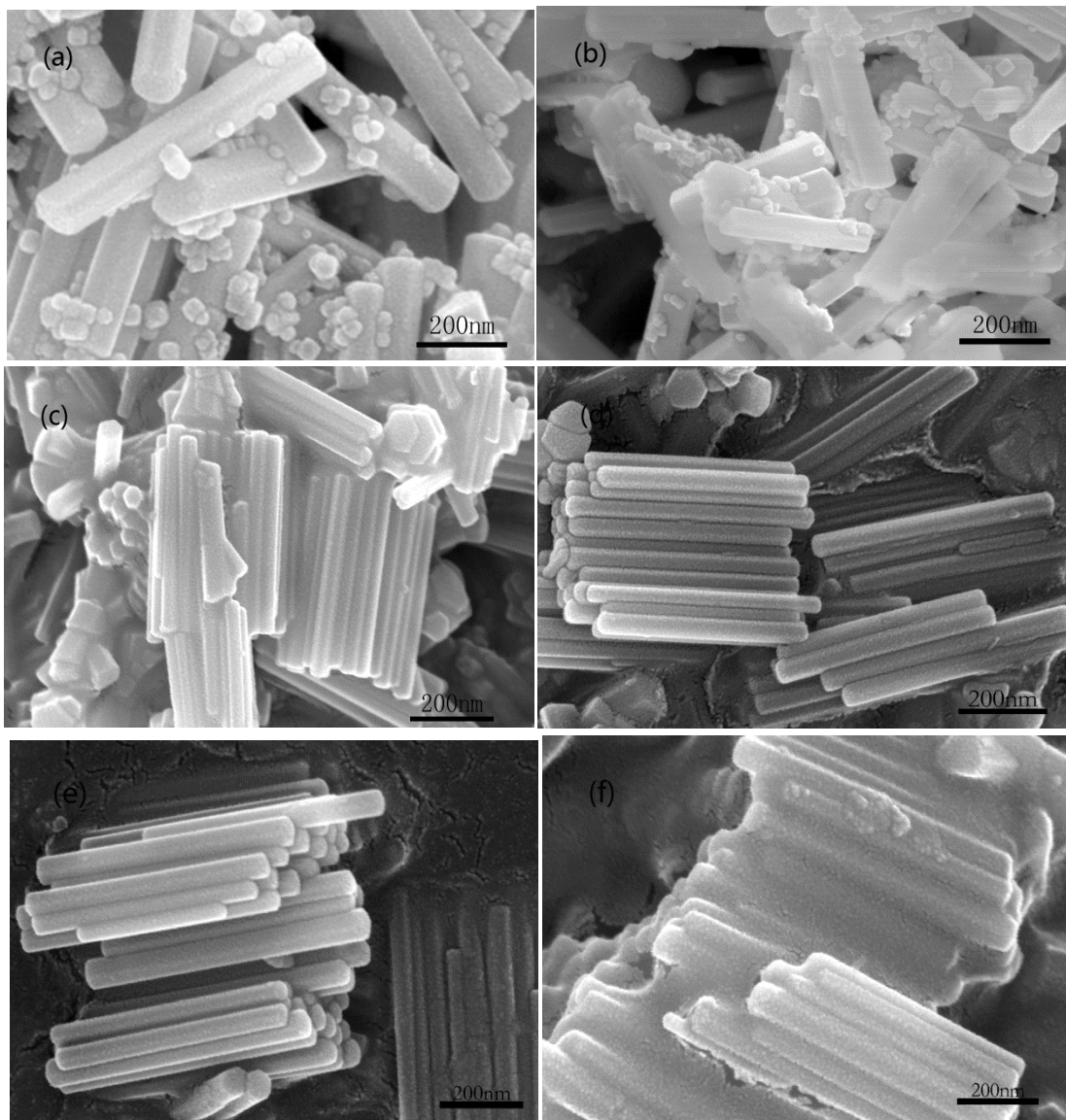


Figure.2 The SEM images of $\text{NaY}_{0.8-x}\text{F}_4:18\%\text{Yb}^{3+}$, $2\%\text{Er}^{3+}$, $x\%\text{Bi}^{3+}$ ($x = 0, 1, 2, 4, 7, 10\text{mol}\%$): (a) 0 mol%, (b) 1.0 mol%, (c) 3.0 mol%, (d) 4.0 mol%, (e) 7.0 mol% and (f) 10.0 mol%.

As shown in Figure. 3(a), the UC spectra of $\text{NaY}_{0.8-x}\text{F}_4:18\%\text{Yb}^{3+}, 2\%\text{Er}^{3+}, x\%\text{Bi}^{3+}$ ($x = 0, 1, 2, 4, 7, 10\text{mol}\%$) exhibited three emission bands at peak 522nm, 543nm (green) and 655 nm (red), which derived from the transitions between the energy levels ($^2\text{H}_{11/2}, ^4\text{S}_{3/2}$) \rightarrow $^4\text{I}_{15/2}$ and $^4\text{F}_{9/2}\rightarrow$ $^4\text{I}_{15/2}$ of Er^{3+} , respectively^[15]. It can be found with the increase of the doping ion concentration, the intensity of green emission and red emission on NaYF_4 have changed greatly. When Bi^{3+} doping concentration is 4 mol%, the red and green emissions reached the maximum value. After that, the UC intensity decreases and even quenches. Connection with Figure.1, The effect of Bi^{3+} ions on the lattice is mainly substitutional doping, which increases the distance between the crystal planes of the ions and leads to the increase of the distance between the energy centers and the central ions of the Er^{3+} ions. In comparison with the increase of the crystal spacing caused by the ionic radius and the decrease of energy transfer, the 4f resonance transition has a greater enhance on the UC luminescence of NaYF_4 ^[16]. Therefore, the intensity of UC emission has increased. As indicated in Figure. 3(b), when 4 mol% Bi^{3+} is doped, the intensity of red and green emission is enhanced by 5.5 and 4.9 times, respectively. In addition, the intensity ratio of red to green emission is found to be approximately equal to 1 at different level of Bi^{3+} ions. Hence, it can be concluded that the influence of Bi^{3+} doping on the UC materials intensity of Er^{3+} is relatively constant^[17].

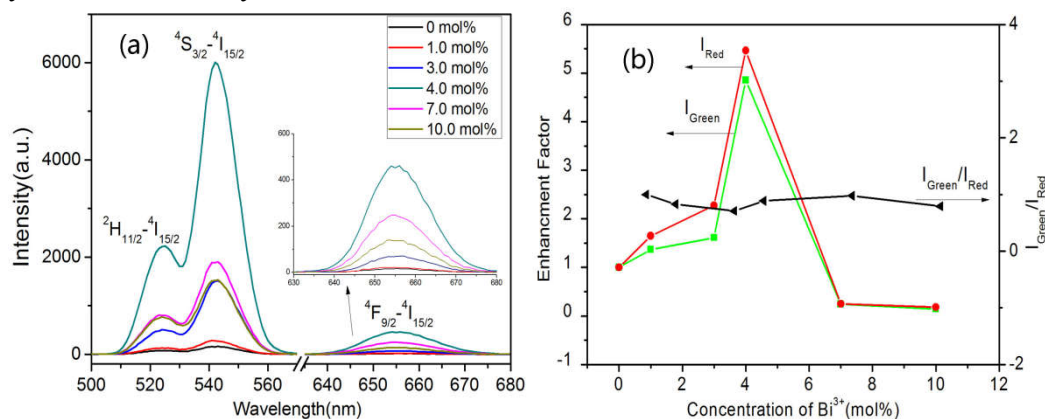


Figure. 3(a): UC luminescence spectra of the samples $\text{NaY}_{0.8-x}\text{F}_4:18\%\text{Yb}^{3+}, 2\%\text{Er}^{3+}, x\%\text{Bi}^{3+}$ ($x = 0, 1, 2, 4, 7, 10\text{mol}\%$) under 980 nm excitation and Figure. 3(b): Enhancement factors of the green, red and total up-conversion emissions of $\text{NaY}_{0.8-x}\text{F}_4:18\%\text{Yb}^{3+}, 2\%\text{Er}^{3+}, x\%\text{Bi}^{3+}$ ($x = 0, 1, 2, 4, 7, 10\text{mol}\%$) crystals as a function of Bi^{3+} concentrations (The integrated intensity of Bi^{3+} -free sample was scaled as unit, excitation at 980 nm).

4. Conclusion

In conclusion, we have prepared a series of $\text{NaY}_{0.8-x}\text{F}_4:18\%\text{Yb}^{3+}, 2\%\text{Er}^{3+}, x\%\text{Bi}^{3+}$ ($x = 0 \sim 10\%$) crystals through a simple hydrothermal method. The phase purity and UC intensity of $\text{NaYF}_4:\text{Yb}^{3+}, \text{Er}^{3+}$ crystals were controlled by doping different concentrations of Bi^{3+} . Compared to Bi^{3+} -free samples, when incorporating 4.0 mol% Bi^{3+} ion, the UC red and green emission intensity was increased by a factor of 5.5 and 4.9, respectively, which was mainly due to modification of the crystal symmetry of Er^{3+} by the Bi^{3+} doping.

5. Acknowledgments

This work is supported by NSFC (51362002), Natural Science Foundation of Jiangxi Province

(20161BAB203098, 20171BAB206016), Key Research and Development Projects of Jiangxi Province (20171BBH80021), Education Department of Jiangxi Province (GJJ150599, GJJ150583), and the financial supports from Jiangxi Key Laboratory for Mass Spectrometry and Instrumentation (JXMS201506) are also greatly appreciated.

References

- [1] Wang, M.; Wu, J.; Chen, Z., *Key Engineering Materials*, (2016) **703**, 242.
- [2] Tan, G. R.; Wang, M.; Hsu, C. Y.; Chen, N.; Zhang, Y., *Advanced Optical Materials*, (2016) **4**, 984.
- [3] Méndez-Ramos, J.; Ruiz-Morales, J. C.; Acosta-Mora, P.; Khaidukov, N., *Journal of Materials Chemistry C*, (2016) **4**, 801.
- [4] Tian, X.; Wei, X.; Chen, Y.; Duan, C.; Yin, M., *Opt Express*, (2014) **22**, 30333.
- [5] Shan, G. B.; Demopoulos, G. P., *Advanced materials*, (2010) **22**, 4373.
- [6] Trindade, T.; O'Brien, P.; Pickett, N. L., *Chem Mater*, (2001) **13**, 3843.
- [7] Chen, D.; Wang, Y., *Nanoscale*, (2013) **5**, 4621.
- [8] Boyer, J. C.; Cuccia, L. A.; Capobianco, J. A., *Nano Letters*, (2007) **7**, 847.
- [9] He, E.; Zheng, H.; Gao, W.; Tu, Y.; Lu, Y.; Tian, H.; Li, G., *Journal of Nanoscience & Nanotechnology*, (2014) **14**, 4139.
- [10] Lei, L.; Chen, D.; Xu, J.; Zhang, R.; Wang, Y., *Chemistry – An Asian Journal*, (2014) **9**, 728.
- [11] Kumar, D.; Verma, K.; Verma, S.; Chaudhary, B.; Som, S.; Sharma, V.; Kumar, V.; Swart, H. C., *Physica B Condensed Matter*, (2017),
- [12] Liang, Z.; Cui, Y.; Zhao, S.; Tian, L.; Zhang, J.; Xu, Z., *Journal of Alloys & Compounds*, (2014) **610**, 432.
- [13] Shannon, R. D., *Acta Crystallogr A*, (1976) **A32**, 751.
- [14] Wang, C.; Cheng, X., *Journal of Alloys & Compounds*, (2015) **649**, 196.
- [15] Rai, M.; Singh, S. K.; Singh, A. K.; Prasad, R.; Koch, B.; Mishra, K.; Rai, S. B., *ACS Applied Materials & Interfaces*, (2015) **7**, 15339.
- [16] Liang, Z.-Q.; Zhao, S.-L.; Cui, Y.; Tian, L.-J.; Zhang, J.-J.; Xu, Z., *Chinese Physics B*, (2015) **24**, 037801.
- [17] Chen, Z.; Wang, M.; Wang, H.; Le, Z.; Huang, G.; Zou, L.; Liu, Z.; Wang, D.; Wang, Q.; Gong, W., *Journal of Alloys & Compounds*, (2014) **608**, 165.